Solar Energy Materials and Solar Cells 172 (2017) 293–300

Contents lists available at ScienceDirect

Solar Energy Materials and Solar Cells

journal homepage: www.elsevier.com/locate/solmat

Evidence of an identical firing-activated carrier-induced defect in monocrystalline and multicrystalline silicon

Daniel Chen[a,*,1], Moonyong Kim[a,1], Bruno V. Stefani[a,b], Brett J. Hallam[a], Malcolm D. Abbott[a], Catherine E. Chan[a], Ran Chen[a], David N.R. Payne[a], Nitin Nampalli[a], Alison Ciesla[a], Tsun H. Fung[a], Kyung Kim[a], Stuart R. Wenham[a]

[a] School of Photovoltaic and Renewable Energy Engineering, University of New South Wales, Kensington, NSW 2052, Australia
[b] School of Engineering, Federal University of Rio Grande do Sul, Porto Alegre 90040-060, Brazil

ARTICLE INFO

Keywords:
Carrier-induced degradation (CID)
LETID
Multicrystalline silicon (mc-Si)
Monocrystalline silicon (c-Si)
Degradation
Hydrogen

ABSTRACT

While progress has been made in understanding the behaviour of the recently identified carrier-induced degradation mechanism in p-type multicrystalline silicon solar cells, little is currently known about the root cause of the defect or its possible existence in other materials. In this work, we present evidence suggesting that the defect also exists in Czochralski grown monocrystalline silicon wafers. For both mono- and multicrystalline silicon we demonstrate: 1) the presence of a degradation and recovery of bulk minority carrier lifetime induced by either illuminated or dark annealing; 2) a modulation in the magnitude of degradation by varying the firing conditions; and 3) capture cross-section ratios of 39.4 ± 4.9 and 33.4 ± 1.5 in monocrystalline and multicrystalline silicon, respectively. The results indicate that the recently identified degradation mechanism does not only occur in multicrystalline silicon from illuminated annealing at elevated temperatures, but it is also induced by dark annealing at elevated temperatures, and that the degradation can occur in Czochralski grown silicon.

1. Introduction

Performance degradation due to the presence of metastable bulk defects is a key area of research within the photovoltaic community. The formation of these defects under conditions similar to solar cells operating conditions in the field, can result in a reduction of as much as 10% relative efficiency on monocrystalline silicon (c-Si) [1] and up to 16% relative efficiency in multicrystalline silicon (mc-Si) [2]. Given that the degradation occurs from exposure to illumination, such degradation mechanisms are often referred to as light-induced-degradation (LID) mechanisms, however more correctly, the illumination generates excess carriers, which in turn leads to defect formation. Hence these are actually carrier-induced degradation (CID) mechanisms. The root cause of CID in Czochralski (Cz) grown c-Si wafers containing boron and oxygen has been identified as the formation of boron-oxygen (BO) defects although the actual composition of the defect is not yet understood. In mc-Si, the root cause for a recently identified degradation mechanism [3] has not yet been determined and this remains an area of intense research.

There are a number of key behaviours that distinguish this degradation mechanism in mc-Si from other well-known degradation mechanisms in silicon. Firstly, unlike BO defects, a high-temperature firing process is required to activate the degradation which then occurs during subsequent illuminated annealing [4–6]. Secondly, the degradation in mc-Si is not typically observed within experimental timescales at room temperature. Generally, an elevated temperature of at least 75 °C is used to highlight this degradation mechanism. As a result, some studies have used the label “Light and Elevated Temperature Induced Degradation” (LeTID) to describe this effect [4,7–10]. At 75 °C, the degradation can take 100 h, and the subsequent recovery can take 700 h [10,11]. With these extremely long time constants; a recovery out in the field would occur on a timescale equivalent to decades [10]. Thirdly, the degradation has also been observed in gallium doped wafers, hence excluding BO defects or iron-boron (Fe-B) pairs as possible defect candidates [3,12]. Due to the significant difference in the known kinetics and defect properties of copper-related degradation [13], copper-related degradation can also be ruled out.

A number of possible root causes for the CID in mc-Si have been proposed. These include the possible involvement of hydrogen, or the dissociation of deep-level point defects, which contribute to changes in recombination activity [4,8]. There appears to be a growing consensus that hydrogen plays a key role in the activation of the defect

* Corresponding author.
E-mail address: daniel.chen@unsw.edu.au (D. Chen).
[1] These authors have contributed equally to this work.

http://dx.doi.org/10.1016/j.solmat.2017.08.003
Received 27 June 2017; Received in revised form 1 August 2017; Accepted 2 August 2017

Table 1
Peak firing zone set-point temperatures of the Schmid fast-firing furnace with corresponding actual measured peak wafer temperatures.

Set-point (°C)	500	600	700	800	855	900
Peak actual (°C)	440 ± 3.0	501 ± 2.0	598 ± 2.0	715 ± 6.0	744 ± 4.5	815 ± 3.0

[4,7,11,14,15]. Extensive analysis of Shockley-Read-Hall (SRH) statistics [16] of the defect has been attempted. Injection-dependent lifetime spectroscopy (IDLS) measurements have identified a bulk defect with capture cross-section ratios of approximately $26 < k < 36$ assuming a mid-gap defect energy level [4,7,8]. However, other values, both higher and lower, have also been reported [6,17]. Various studies targeting the elimination or suppression of this degradation have been presented [5,9,12]. The application of standard treatments for the passivation of BO defects have shown to assist in a partial suppression of the degradation extent, however extended light soaking over hundreds of hours demonstrated a gradual instability in performance [12,18].

More recently, pre-dark annealing at elevated temperatures has been shown to modulate the kinetics of the degradation [11,19]. In particular, dark annealing was shown to change the degradation rate, extent of CID and the subsequent rate of recovery under illumination. Although it has been demonstrated that dark annealing may induce a surface instability of the passivating dielectrics resulting in a drop in carrier lifetime [20], in some cases, a homogeneous degradation in the bulk under carrier injection has been shown [4]. Recently, we demonstrated that sufficient dark annealing at elevated temperature resulted in degradation of the open-circuit voltage of mc-Si solar cells. It was suggested that this degradation may be due to thermally-induced CID [11].

Typically, it has been assumed that this defect only occurs in mc-Si, as no significant degradation with illumination at elevated temperatures was observed in c-Si silicon in early studies, beyond that expected for BO related degradation [3]. This has resulted in the vast majority of work investigating the defect in mc-Si. However, recent work by Nampalli et al. and Fertig et al. indicated that similar metastable defects may also exist in solar grade Cz silicon wafers [21,22], with an instability in the material beyond that induced by the formation of BO defects. In the study by Fertig et al., measurements were carried out on modules and no attempts were made to identify the recombination properties of the defect. A degradation of bulk lifetime has also been observed in p-type float-zoned (FZ) material with similar recombination properties [23]. Hence it is unclear whether or not the degradation mechanism observed in p-type mc-Si is also present in other materials such as FZ or Cz silicon.

This paper presents experimental evidence that the defect responsible for carrier-induced degradation in mc-Si, typically termed 'LeTID', can also be found in Cz substrates. Furthermore, we demonstrate the existence of a purely thermal degradation and regeneration mechanism with a similar behaviour to the light-induced counterpart on both mc-Si and c-Si silicon wafers. Given the differences between the substrates, these results provide important insights into the possible root cause of the defect. Furthermore, it has important implications for the long-term stability of PERC solar cells created on Cz silicon.

2. Experimental details

To carry out our investigation of carrier-induced degradation, commercially available multicrystalline and Czochralski grown wafers were obtained from GCL-Poly and LONGi Silicon respectively. 1.7 ± 0.2 Ω cm *p*-type boron-doped high performance (HP) multicrystalline wafers were used, with dimensions 156 mm × 156 mm. The mc-Si wafers were chosen from adjacent positions in the ingot to ensure comparable electrical and crystallographic properties. Similarly, neighbouring 1.6 ± 0.1 Ω cm Czochralski (Cz) grown boron-doped *p*-type monocrystalline wafers were used (156 mm × 156 mm). Mc-Si wafers underwent standard industrial acidic texturing. The monocrystalline wafers (c-Si) received saw damage etch followed by a 40 Ω/□ gettering diffusion prior to a 2 µm alkaline texturing etch on each side. The final thickness of all wafers was 180 ± 3 µm. A $POCl_3$ diffusion was performed on all wafers resulting in a n^+-emitter layer on each side ($R_{sheet} \approx 65\Omega/\square$). Passivating hydrogenated silicon nitride (SiN_x:H) dielectric layers with a 2.08 refractive index at 633 nm [24,25] and thickness of 75 nm were realized on both sides using a Roth & Rau MAiA remote plasma-enhanced chemical vapor deposition tool (r-PECVD) to form symmetrical lifetime structures. Wafers were laser cleaved into tokens (52 mm × 52 mm) and assorted into identical 'sister' sets. Tokens in a single set of each material with the exception of an unfired control sample were fired at a series of peak set-point temperatures ranging between 500 °C and 900 °C. The wafer temperature profiles were measured using a Q18 Datapaq thermal profiler and resulted in a range in peak actual temperature between 440 ± 3 °C and 815 ± 3 °C (see Table 1) at a constant belt speed of 4.5 m/s in a commercial Schmid fast-firing metallization furnace.

All tokens were then annealed in the dark on a hotplate at 175 ± 2 °C (actual temperature). To investigate whether the defect induced through dark annealing was identical to that commonly found under illumination, 'sister' tokens processed in the identical manner were tested for their response to illuminated annealing. Samples were exposed to an illumination intensity of approximately 0.98 ± 0.05 kW/m^2 (S305C, Thorlabs) supplied by four broadband halogen sources while on a hotplate at 175 ± 3 °C.

The evolutions in carrier lifetime during degradation and subsequent recovery was monitored periodically by ex-situ means using a quasi-steady-state photoconductance tool (QSS-PC) (Sinton Instruments WCT-120) and analysed using the generalized method as proposed in [26] and references therein. Measured data was corrected for Auger recombination using the Richter model [27]. Effective minority carrier lifetimes (τ_{eff}) were extracted at an excess minority carrier density (Δn) of 9.1 × 10^{14} /cm^3 (equal to approximately 10% of the background boron dopant density). Given the difference in starting carrier lifetimes, the normalised defect density (*NDD*) was determined using the following equation [28]:

$$NDD(\Delta n) = \sigma_n v_n N_t = \frac{1}{\tau_{DA}(\Delta n)} - \frac{1}{\tau_{fired}(\Delta n)},$$

where σ_n is the electron capture cross section of the defect, v_n is the thermal velocity of electrons and N_t is the defect concentration.

Injection-dependent Shockley-Read-Hall (SRH) lifetimes ($\tau_{SRH}(\Delta n)$) of the defect were realized by the difference between inverse carrier lifetimes after firing ($\tau_{fired}(\Delta n)^{-1}$) and after degradation ($\tau_{degraded}(\Delta n)^{-1}$):

$$\tau_{SRH}(\Delta n)^{-1} = \tau_{degraded}(\Delta n)^{-1} - \tau_{fired}(\Delta n)^{-1}$$

For the purpose of this study, we denote $\tau_{degraded}(\Delta n)^{-1}$ as $\tau_{DA}{}^{-1}$ and $\tau_{LS}{}^{-1}$ for samples degraded using dark annealing and light soaking respectively. By using this approach, we assume that other recombination mechanisms, bulk carrier lifetimes ($\tau_{bulk}{}^{-1}$) and any defects intrinsic to the samples after firing remain identical in both conditions. Although changes in lifetime were assumed to be dominated by the defect under investigation, other defects may be modulated by processes used and need to be considered. In particular, precautions were taken to reduce the impact of other carrier-activated defects. For each measurement, samples were left in the dark for > 3 h at room temperature to minimise any potential influence by interstitial iron (Fe_i) and allow the reformation of Fe-B pairs. By using a dark annealing condition, the activation of recombination active BO defect was also

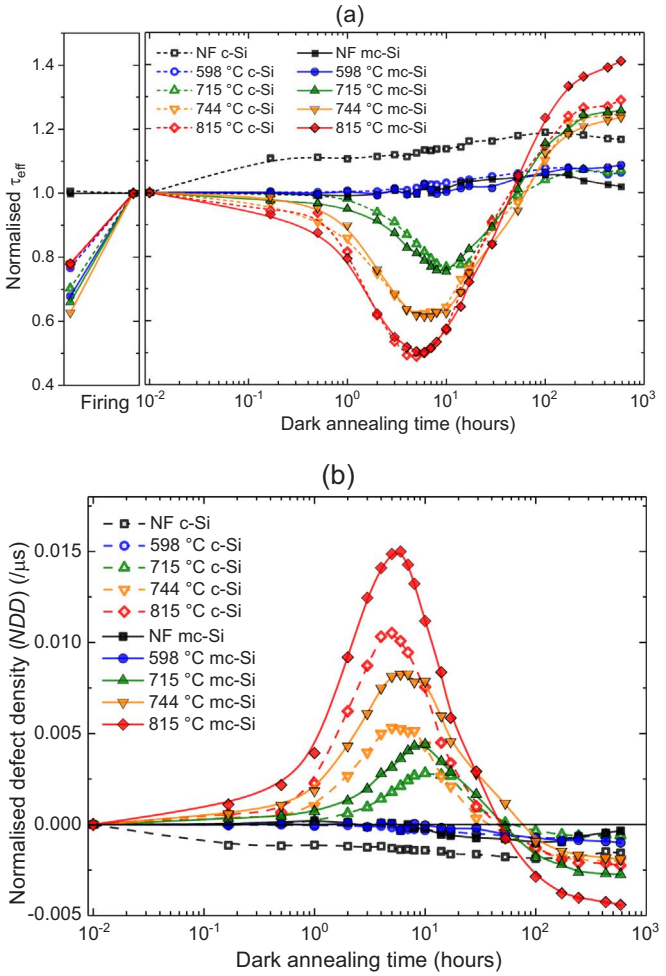

Fig. 1. (a) Normalised effective minority carrier lifetime (to the value directly after firing) vs. dark annealing duration at 175 °C of fired (from 598 °C to 815 °C) and not fired (NF) monocrystalline (c-Si) (solid lines) and multicrystalline (mc-Si) (dashed lines) silicon wafers. The additional left section portrays the relative changes in lifetime due to firing. Lifetimes were extracted at an injection level of $\Delta n = 9.1 \times 10^{14}$ /cm^3. Lines are shown to serve as a guide to the eye. (b) Corresponding normalised defect density as a function of dark annealing time.

avoided. To further minimise errors, the dark saturation current densities (J_{0E}) of both states were quantified and monitored for changes. A Chi-square analysis was undertaken to evaluate the quality of fit and determine the range for defect k-values [29].

3. Experimental results

3.1. Impact of firing temperature on defect formation in the dark

The evolution of the effective minority carrier lifetime of the samples, normalised to that after firing, is shown in Fig. 1(a), as a function of the dark annealing duration post-firing. The corresponding plot of *NDD* is shown in Fig. 1(b), to account for the differences in absolute lifetimes between the two materials. Both the c-Si samples (open symbols) and the mc-Si samples (closed symbols) show a degradation and recovery in minority carrier lifetime, corresponding to a rise and then fall for the normalised defect density. A notable behaviour with dark annealing was the apparent time scales of defect formation and recovery present in both mc-Si and Cz samples. Although not identical, these were extremely similar for the two materials. For the highest peak firing temperature (815 °C), the maximum defect concentration occurred at approximately 5 h of dark annealing, however, at 715 °C, the time scale was extended to approximately 10 h. In both materials, the maximum *NDD* was dependent on the peak firing temperature, with increased firing temperatures resulting in an increased extent of degradation. Samples fired at temperatures below 598 °C (not shown) either did not degrade, or showed a slight improvement in lifetime of up to 5% relative upon annealing. The maximum *NDD* varied between the two materials, with c-Si materials consistently reaching a lower maximum *NDD* than that for mc-Si. Both the non-fired mc-Si and c-Si control samples showed no significant changes due to dark annealing, however c-Si samples saw a slight improvement within the first 10 min of dark annealing. Further annealing of all degraded samples resulted in a recovery of lifetime, arriving back to the initial pre-dark annealed state after approximately 40 h. Unlike the degradation time constant and magnitude, the recovery time constant appeared to be unchanged by the firing condition. With continued annealing up to 584 h, an increase in carrier lifetime of up to 40% was observed on some samples, with the magnitude of recovery in mc-Si samples being greater than that of c-Si samples.

The initial increase in carrier lifetime of the non-fired c-Si control sample during dark annealing is likely due to the dissociation of pre-existing BO defects into their recombination inactive state [30,31]. It is likely that a small concentration of BO defects had formed before characterisation, while under ambient light in the laboratory. No subsequent degradation of the non-fired sample was observed during dark annealing, which indicates that BO defect complexes cannot effectively form through dark annealing.

To further illustrate the similarities in firing dependence and degradation extent, Fig. 2 shows the maximum relative magnitude in degradation (blue) and the absolute effective minority carrier lifetimes after firing (black) and at the minima in the cycle (red) as a function of firing temperatures. The maximum degradation extent increased significantly between the temperatures of 598 °C and 715 °C, consistent with the results of Chan et al. in the study of CID in mc-Si [5]. It was also observed that a peak in carrier lifetime occurred using a peak firing temperature of 715 °C. For higher firing temperatures, the lifetime enhancements due to firing were reduced.

It is important to note that the behaviours presented above can be very specific to our substrate materials. To confirm whether similarities in the defect behaviours such as the normalised degradation extent were coincidental or due to the specific source of wafers, future work would involve using wafers from a range of different manufacturers as well as numerous types of Cz wafers.

3.2. SRH analysis of mc-Si and c-Si

In the previous section, we identified a lifetime limiting degradation mechanism with similar characteristics in both mc-Si and c-Si wafers. In this section, we carry out IDLS analysis on the measured lifetimes of both materials; 1) after firing at 815 °C; and 2) at the maximum degradation extent (after approximately 5 h of dark annealing) (see Fig. 3). Dark annealing was found to cause no notable change in J_{0E} after firing ($J_{0E,fired}$) and in the degraded state ($J_{0E,DA}$), which indicates the degradation due to annealing was not caused by an instability of the surface dielectric layers. An energy level of mid-gap was chosen to evaluate the defect characteristics as the exact energy level remains unknown, and a large range of defect energy levels (with a sufficient distance from the band edges) result in recombination properties similar to that of a mid-gap defect. The measured capture cross-section ratio, k, of the defects formed by dark annealing on mc-Si (Fig. 3(a)) and on c-Si (Fig. 3(b)) were $k_{DA} = 33.4 \pm 1.4$ and $k_{DA} = 39.4 \pm 4.9$, respectively. These results are similar to values previously derived in other work for the defect in mc-Si and FZ materials with illuminated annealing processes [7,8,23,32].

It is also important to note that the extracted defect k-values could also be fitted to the SRH lifetimes measured directly after firing, suggesting a possible preformation of the defect during firing. In Fig. 4, we show the fitted inverse carrier lifetime data for mc-Si samples before

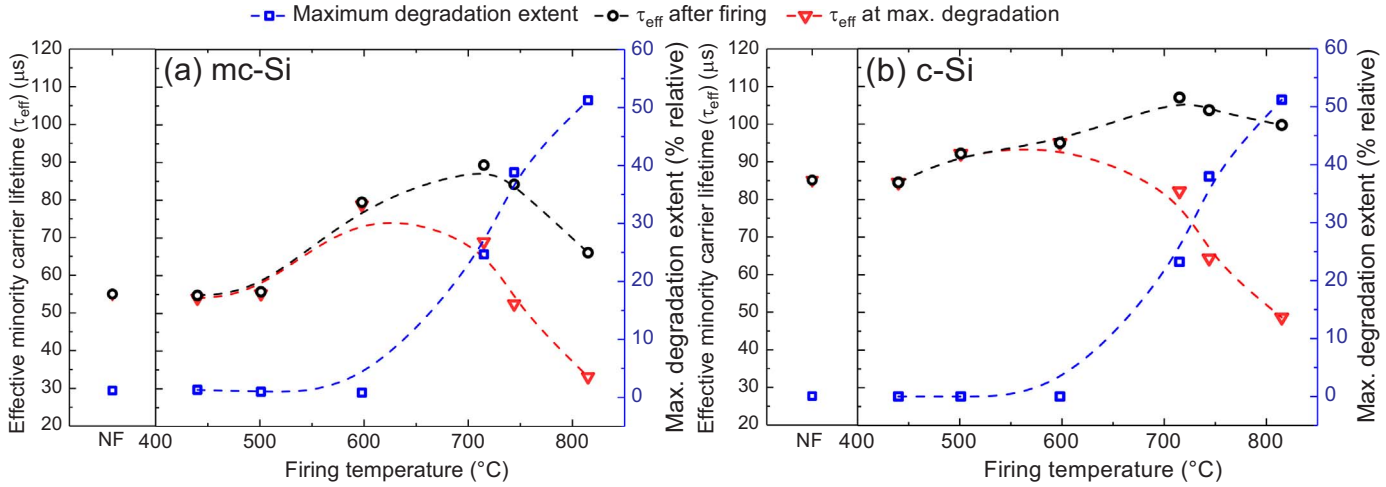

Fig. 2. The effective lifetime measured after firing (black) and at maximum degradation (red) as a function of firing temperature for (a) mc-Si and (b) c-Si samples. The maximum degradation extent (blue) is displayed on the secondary y-axis. Lifetimes were extracted at an injection level of $\Delta n = 9.1 \times 10^{14}$ /cm^3. Dashed lines serve as a guide to the eyes. (For interpretation of the references to color in this figure legend, the reader is referred to the web version of this article).

and after firing at 598 °C and 815 °C. At the higher temperature of 815 °C (shown in green), there is an indication of SRH recombination brought about by a defect with a *k*-value of 33.4 ± 1.5. At the lower temperature of 598 °C (shown in red), there is no evidence of such firing-activated recombination. For the c-Si samples, a *k*-value of approximately 32.3 ± 5.3 was also observed (not shown).

3.3. Comparison of light and thermally generated defects

We compared the IDLS results from samples degraded using dark annealing to those degraded in the light at elevated temperatures. Fig. 5(a) shows the minority carrier lifetime as a function of illuminated annealing time for mc-Si samples. Similar trends were observed to those caused by dark annealing. The degradation extent exhibited through illuminated annealing was again, highly dependent on the peak firing temperature. A similar behaviour in recovery was also observed. With the added illumination, the degradation was greatly accelerated, with samples fired at 815 °C reaching a minimum after approximately 15 min, as opposed to 5 h for dark annealing. The recovery of all samples was also greatly accelerated, with complete recovery to their pre-degraded states after approximately 900 min (15 h). The IDLS analysis of the defect in Fig. 5(b) for mc-Si also identified SRH

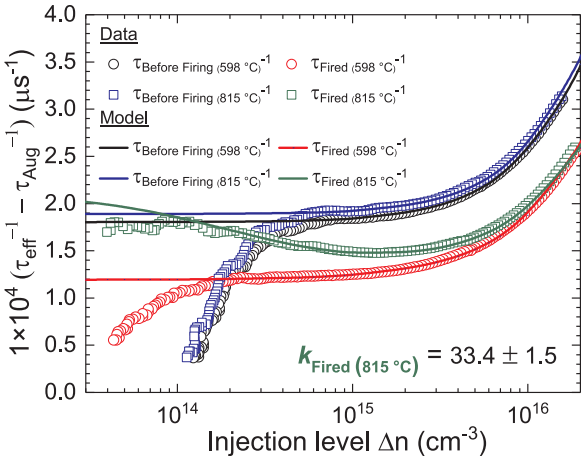

Fig. 4. Measured IDLS results for mc-Si sister wafers prior to and after fast-firing at 598 °C and 815 °C. Solid lines show the fitted lifetime curves. (For interpretation of the references to color in this figure, the reader is referred to the web version of this article).

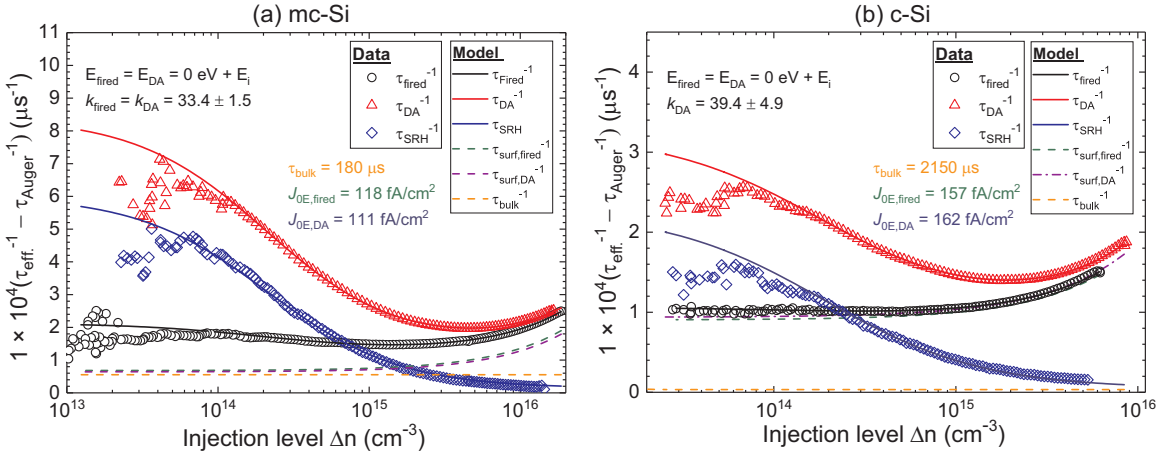

Fig. 3. IDLS data showing measured injection dependent inverse minority carrier lifetime for (a) mc-Si and (b) c-Si samples directly after firing at 815 °C (τ_{fired}^{-1}) (black circles) and after degradation due to dark annealing (τ_{DA}^{-1}) (red triangles) at 175 ± 2 °C. The inverse SRH lifetime (τ_{SRH}^{-1}) is depicted using blue diamonds. The fitted lifetime components are indicated by the solid coloured lines: τ_{fired}^{-1} (black), τ_{DA}^{-1} (red) and τ_{SRH}^{-1} (blue). Other fit metrics for the surface and bulk components are indicated by the dotted lines: $\tau_{surf,fired}^{-1}$ (green), $\tau_{surf,DA}^{-1}$ (purple) and τ_{bulk}^{-1}(orange). (For interpretation of the references to color in this figure legend, the reader is referred to the web version of this article).

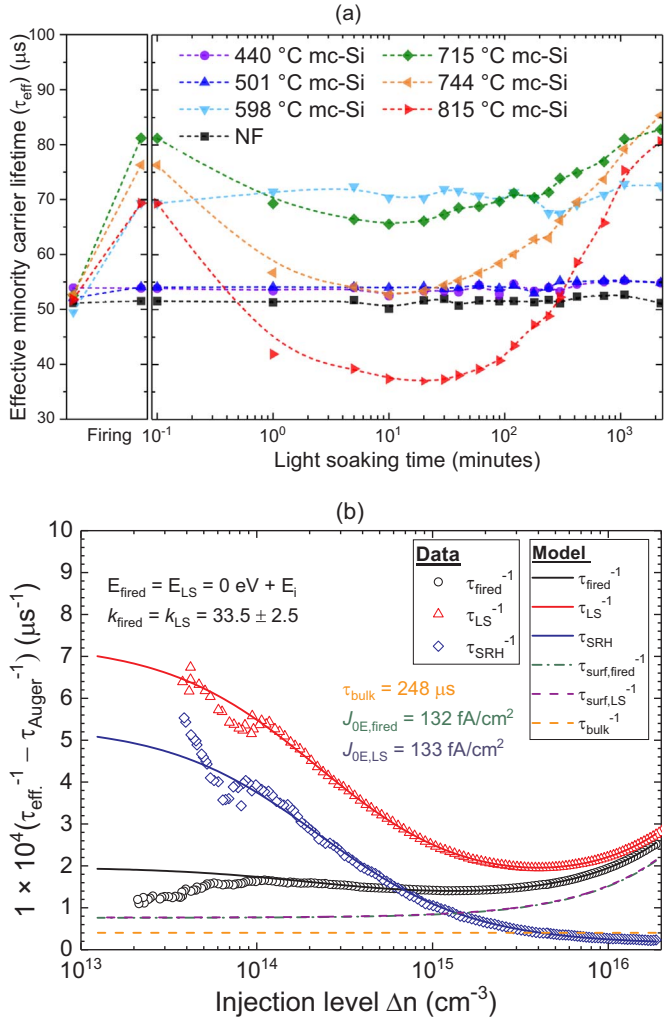

Fig. 5. (a) Absolute change in effective minority carrier lifetime extracted at an injection level of $\Delta n = 9.1 \times 10^{14}$ /cm^3 of mc-Si samples fired at various temperatures as the result of illuminated annealing. Dashed lines serve as a guide to the eye. (b) IDLS data showing the inverse minority carrier lifetime for a mc-Si sample directly after firing (τ_{fired}^{-1}) (black circles) at 815 °C and after degradation due to illuminated annealing (τ_{LS}^{-1}) (red triangles) at 175 ± 3 °C and 0.98 ± 0.05 kW/m^2. The fitted lifetime components are indicated by the solid coloured lines: τ_{Fired}^{-1} (black), τ_{LS}^{-1} (red) and τ_{SRH}^{-1} (blue). Other fit metrics for the surface and bulk components are indicated by the dotted lines: $\tau_{surf,fired}^{-1}$ (green), $\tau_{surf,LS}^{-1}$ (purple) and τ_{bulk}^{-1} (orange). (For interpretation of the references to color in this figure legend, the reader is referred to the web version of this article).

recombination with a *k*-value of $k_{LS} = 33.5 \pm 2.5$, which strongly suggests that the defects activated through both dark annealing and illuminated annealing are identical. Hence, it is quite likely that thermally generated carriers at elevated temperatures play a similar role in stimulating degradation as the carriers generated by illumination.

Although degradation was observed under illumination in c-Si beyond that expected from BO defects (not shown), it was difficult to ascertain the minima point in degradation under illumination. This was due to the complications from BO defects including the simultaneous defect formation and passivation reactions. An estimation assuming a single defect resulted in a *k*-value of 36.6 ± 2.1 for a firing temperature of 815 °C, compared to a value of 11.4 ± 0.6 on the non-fired sample, related to BO defects. Further details on this will be presented in a future work.

4. Discussion

In the previous sections, IDLS measurements and degradation behaviour demonstrated experimentally that the defect responsible for the severe degradation of minority carrier lifetime in mc-Si (typically called LeTID) can also occur in solar grade Cz Si material. Furthermore, the minimal changes in surface passivation quality of both materials suggests that the degradation arises as the result of bulk defect formation rather than surface instability. The authors would like to note that although samples were given different treatments such as texturing which may affect light trapping and surface passivation, the majority of processing steps were identical including the silicon nitride deposition and firing processes. Nonetheless, the presence of similar trends in degradation behaviour on vastly dissimilar materials may shed light on the validity of various hypotheses regarding the defect kinetics and identify probable root causes.

4.1. Interpretation of defect kinetics

4.1.1. Firing dependence

The observed trends in carrier lifetime and degradation extent due to fast-firing with both illuminated and dark annealing follow a similar behaviour to those presented by numerous others studying CID in mc-Si [5,6,15]. Bredemeier et al. and Chan et al. both demonstrated a modulation of the degradation extent during light soaking due to differences in peak fast-firing temperature. We demonstrate similar trends when light soaking was performed at the elevated temperature of 175 °C. However, due to the higher temperature for the illuminated anneal, the degradation and recovery reactions occurred at an accelerated rate.

The decline in lifetime enhancement from firing at high temperatures (> 715 °C) is not a new phenomenon either. For example, it has been shown that post-diffusion oxidation processes, annealing in nitrogen and fast firing can cause severe bulk 'poisoning', which worsened at increased processing temperatures [33–37]. Although we cannot be certain that the phenomenon observed in other studies is identical, with the determined SRH parameters after firing, we conclude that a pre-formation of the defect under investigation is the likely cause for the degradation at elevated fast-firing temperatures observed in this work.

The increase in extent of degradation with increasing peak firing temperature suggests that firing leads to a formation of defect precursors. However, the shift in the degradation time constant, suggests that in addition, the firing process can lead to a thermal evolution of the defects. These defects can also be activated by subsequent light soaking or dark annealing. It should be noted that this paper has not explored whether this pre-formation is due to the rate of cooling, total thermal budget or simply the peak firing temperature.

4.1.2. Thermal generation of CID

Degradation in mc-Si wafers and solar cells has typically been activated by excess carrier generation through illumination or current injection [18,38]. Furthermore, dark annealing has been used on degraded samples to result in a metastable recovery of carrier lifetime, presumably causing a temporary annihilation of the defect [39]. Recently, we demonstrated that the degradation of minority carrier lifetime could also be induced by dark annealing [11]. It was claimed that the degradation could be due to the thermal generation of minority carriers. For example, increasing the temperature from 75 °C to 175 °C can increase the concentration of thermally generated electrons by four orders of magnitude. This can have a significant impact on charge state concentrations of impurities in silicon, such as interstitial hydrogen [40]. Hence, the increase in temperature can explain the ability to form defects in the dark. It is likely that a similar mechanism takes places for the pre-formation of defects during fast-firing. At these temperatures, further enhancements in minority carrier charge state concentrations will result. Furthermore, the higher temperatures will accelerate the diffusivity of impurities and kinetic reactions, greatly reducing the time required to form defects. Hence, rather than approximately 7 h in the dark at 175 °C, a small concentration of defects can form in a matter of

seconds during fast-firing.

4.1.3. Improvement with prolonged annealing

The improved lifetime of samples after extended dark and illuminated annealing, beyond the starting lifetime, may pertain to the hydrogen passivation of crystallographic defects and impurities, or the annihilation of any defects that had already formed during firing. The relative performance enhancements in mc-Si were greater than c-Si, which can potentially be explained by the larger concentration of defects such as grain boundaries and dislocation clusters in multicrystalline silicon [41]. Although the time scale for such improvement at these conditions would not necessarily be feasible for commercial production, accelerating the degradation and recovery rates by increasing the temperature and/or illumination intensity as demonstrated by Chan et al. may be possible [11].

Overall, given the vast differences between mc-Si and c-Si, such correlations in degradation and recovery behaviour strongly indicate the existence of a fundamental defect that is present in both materials. The possible root causes for such behaviour and its implications will be discussed in the following section.

4.2. Implications for root cause

4.2.1. Hydrogen

A leading hypothesis attuned to our results and as suggested through various other studies would be the influence of hydrogen and its interactions with bulk defects [8,14,23,32,42]. Interstitial hydrogen can be introduced at various concentrations from hydrogenated dielectric layers such as PECVD deposited silicon nitride (SiN_x:H) and aluminium oxide (AlO_x:H) [43–46]. Such in-diffusion of hydrogen is recognized to be firing dependent with larger concentrations injected at higher temperatures [5,14]. We observe that degradation can be activated once the fast-firing peak temperature exceeds ~ 598 °C. This is approximately the temperature around which hydrogen release from the silicon nitride layers is reported to start [47]. Furthermore, at this temperature, a clear passivation of grain boundaries can be observed in photoluminescence images (not shown), confirming the injection of hydrogen into the silicon bulk [35]. A hydrogen based model would explain why numerous studies show severe degradation when wafers are fast-fired in the presence of a dielectric such as hydrogenated silicon nitride (SiN_x:H) or aluminium oxide (AlO_x:H) [20] and a suppression of the degradation when fired in the absence of a hydrogen-containing dielectric layers [42]. This interpretation may also explain why PERC solar cells, which employ additional hydrogen-containing AlO_x:H and SiN_x:H layers on the rear surface experience greater susceptibility to degradation than conventional aluminium back surface field (Al-BSF) solar cells with SiN_x:H only on the front surface [48–51]. Although it is understood that hydrogen can be beneficial in the passivation of defects [52], it is possible that a surplus of excess hydrogen may lead to complications. Further experimental evidence however will be required to verify the involvement of hydrogen as a catalyst for CID.

4.2.2. Metallic impurities

Another suggested hypothesis is that metallic impurities alone are acting as recombination active centres responsible for the degradation. Metallic impurities are well known to getter or precipitate in areas of higher solubility such as grain boundaries or the highly-doped regions during processes such as $POCl_3$ diffusion [53,54]. Subsequent high-temperature firing may induce the dissolution of metallic impurities back into the bulk to form recombination active complexes [15,34–37,55]. Studies using temperature and injection-dependent lifetime analysis have identified possible defect candidates; namely the titanium interstitial double donor ($Ti_i^{+/++}$), the molybdenum interstitial donor ($Mo_i^{0/+}$) and the tungsten substitutional donor ($W_s^{0/+}$) [7,17]. Variations in our processing steps may account for the differences in observed NDD between mc-Si and c-Si. The additional heavy diffusion pre-getter step performed on c-Si wafers may result in a lower metallic impurity concentration remaining in the wafer although such gettering may only segregate the relatively faster diffusing impurities such as Fe and Cu and not those such as Ti. This would agree with the observations of supressed degradation using gettering by Zuschlag et al. [9]. Nonetheless, given the differences in manufacturing process for both materials, and the large possible variations in metallic impurity concentrations, future work would require the characterisation of such impurity concentrations present within our wafers.

Furthermore, recent papers have demonstrated a degradation mechanism in high-lifetime FZ wafers with similar recombination characteristics to those identified in mc-Si [23,32]. If the degradation in high lifetime p-type FZ material is caused by the same defect in p-type multicrystalline and p-type Cz, then it would appear unlikely that a specific metallic impurity would be responsible for the CID.

4.2.3. Previous confusion in BO defect studies

There are several reasons why the degradation mechanism observed in this paper on p-type Cz wafers may have previously been unrecognized or simply evaded detection in many BO defect studies. For example, most studies of the BO complex are conducted on samples after the application of passivating dielectric layers, however prior to any elevated temperature firing process [30,56–58]. In instances where samples were fired, the firing temperature may have been too low to induce a significant extent of degradation. Furthermore, the standard short illumination periods required for BO related studies may not have allowed a significant formation of these defects. In addition, the smaller extent of degradation observed on c-Si than mc-Si may have been hidden amongst other dominant light-induced degradation mechanism such as BO defects, copper (Cu) [59] and interstitial iron (Fe_i) [60–62]. It is also possible that degradation caused by this new mechanism has been attributed to other defects. One possible example is the demonstration of a long-term instability in the open circuit voltage of boron-doped Cz solar cells after the permanent deactivation of BO defects by Herguth et al. under illumination at elevated temperatures [63]. Nonetheless, our understanding of the behaviours of Cz materials through dark annealing allows us to demonstrate that the defect formed during dark annealing is unrelated to the common BO defect, but also allows us to study and compare with the behaviours of mc-Si materials, without interference from other light activated defects such as BO.

5. Conclusion

In this study, a form of CID in mc-Si and c-Si with similar behavioural characteristics in both materials was investigated. We demonstrated that a degradation of bulk lifetime, with a strong dependence on firing temperature can occur in both mc-Si and c-Si under either illuminated or dark annealing. This firing dependence is very similar in behaviour to LeTID in mc-Si. The capture cross-section ratios of the defect that was formed by dark annealing on c-Si and on mc-Si were 39.4 ± 4.9 and 33.4 ± 1.5 respectively, again, extremely similar to the reported values reported for mc-Si CID/LeTID in mc-Si. The results indicate a possible form of CID beyond BO in c-Si, in agreement with Fertig et al. [21], suggesting the possibility of lifetime degradation after BO passivation treatment as previously observed by Herguth et al. [64] Although the degradation has not been directly compared to the quantity of hydrogen in the wafers or associated to any hydrogen-induced defect, experimental results suggest that hydrogen likely plays a significant role.

Acknowledgments

The authors would like to thank Duc Huy Dao, Wing Ki Kylie Chan, Jia Neoh, Rong Deng, Nino Borojevic, Dany Sen, Aref Samadi and Ly Mai who assisted with sample processing and characterisation. This work was supported by the Australian Government through the

Australian Renewable Energy Agency (ARENA: 1-A060), the Australian Centre for Advanced Photovoltaics (ACAP: funding for facilities) and the Australian Research Council (ARC: DECRA - DE170100620). Responsibility for the views, information, or advice expressed herein is not accepted by the Australian Government. The authors would also like to thank the commercial partners of the ARENA 1-A060 advanced hydrogenation project.

References

[1] J. Knobloch, S.W. Glunz, D. Biro, W. Warta, E. Schaffer, W. Wettling, Solar cells with efficiencies above 21% proccessed from Czochroalski grown silicon, in: Proceedings of the 25th IEEE Photovoltaic Specialists Conference Washington, DC IEEE, (1996) 405–408. http://dx.doi.org/10.1109/PVSC.1996.564029.

[2] K. Petter, K. Hubener, F. Kersten, M. Bartzsch, F. Fertig, B. Kloter, J. Muller, Dependence of LeTID on brick height for different wafer suppliers with several resistivities and dopants, in: Proceedings of the 9th Int. Work. Cryst. Silicon Sol. Cells, (2016).

[3] K. Ramspeck, S. Zimmermann, H. Nagel, A. Metz, Y. Gassenbauer, B. Brikmann, A. Seidl, Light induced degradation of rear passivated mc-Si solar cells, in: Proceedings of the 27th European Photovoltaic Solar Energy Conference, (2012) 861–865. http://dx.doi.org/10.4229/27THEUPVSEC2012-2DO.3.4.

[4] K. Nakayashiki, J. Hofstetter, A.E. Morishige, T.T.A. Li, D.B. Needleman, M.A. Jensen, T. Buonassisi, Engineering solutions and root-cause analysis for light-induced degradation in p-type multicrystalline silicon PERC modules, IEEE J. Photovolt. 6 (2016) 860–868, http://dx.doi.org/10.1109/JPHOTOV.2016.2556981.

[5] C.E. Chan, D.N.R. Payne, B.J. Hallam, M.D. Abbott, T.H. Fung, A.M. Wenham, B.S. Tjahjono, S.R. Wenham, Rapid stabilization of high-performance multicrystalline P-type silicon PERC cells, IEEE J. Photovolt. 6 (2016) 1473–1479, http://dx.doi.org/10.1109/JPHOTOV.2016.2606704.

[6] D. Bredemeier, D. Walter, S. Herlufsen, J. Schmidt, Understanding the light-induced lifetime degradation and regeneration in multicrystalline silicon, Energy Procedia 92 (2016) 773–778, http://dx.doi.org/10.1016/j.egypro.2016.07.060.

[7] A.E. Morishige, M.A. Jensen, D.B. Needleman, K. Nakayashiki, J. Hofstetter, T.A. Li, T. Buonassisi, Lifetime spectroscopy investigation of light-induced degradation in p-type multicrystalline silicon PERC, IEEE J. Photovolt. 6 (2016) 1466–1472, http://dx.doi.org/10.1109/JPHOTOV.2016.2606699.

[8] M.A. Jensen, A.E. Morishige, J. Hofstetter, D.B. Needleman, T. Buonassisi, Evolution of LeTID defects in p-type multicrystalline silicon during degradation and regeneration, IEEE J. Photovolt. (2017) 1–8, http://dx.doi.org/10.1109/JPHOTOV.2017.2695496.

[9] A. Zuschlag, D. Skorka, G. Hahn, Degradation and regeneration analysis in mc-Si, in: Proceedings of the Conf. Rec. IEEE Photovolt. Spec. Conf., (2016) 1051–1054. http://dx.doi.org/10.1109/PVSC.2016.7749772.

[10] F. Kersten, P. Engelhart, H.C. Ploigt, A. Stekolnikov, T. Lindner, F. Stenzel, M. Bartzsch, A. Szpeth, K. Petter, J. Heitmann, J.W. Muller, A new mc-Si degradation effect called LeTID, in: Proceedings of the 2015 IEEE 42nd Photovoltaic Specialists Conference (PVSC 2015), (2015). http://dx.doi.org/10.1109/PVSC.2015.7355684.

[11] C. Chan, T.H. Fung, M. Abbott, D. Payne, A. Wenham, B. Hallam, R. Chen, S. Wenham, Modulation of carrier-induced defect kinetics in multi-crystalline silicon PERC cells through dark annealing, Sol. RRL (2017) 1600028, http://dx.doi.org/10.1002/solr.201600028.

[12] D.N.R. Payne, C.E. Chan, B.J. Hallam, B. Hoex, M.D. Abbott, S.R. Wenham, D.M. Bagnall, Acceleration and mitigation of carrier-induced degradation in p-type multi-crystalline silicon, Phys. Status Solidi – Rapid Res. Lett. 10 (2016) 237–241, http://dx.doi.org/10.1002/pssr.201510437.

[13] A. Inglese, J. Lindroos, H. Vahlman, H. Savin, Recombination activity of light-activated copper defects in p -type silicon studied by injection- and temperature-dependent lifetime spectroscopy, J. Appl. Phys. 120 (2016), http://dx.doi.org/10.1063/1.4963121.

[14] R. Eberle, W. Kwapil, F. Schindler, M.C. Schubert, S.W. Glunz, Impact of the firing temperature profile on light induced degradation of multicrystalline silicon, Phys. Status Solidi – Rapid Res. Lett. 5 (2016) 1–5, http://dx.doi.org/10.1002/pssr.201600272.

[15] D. Bredemeier, D. Walter, S. Herlufsen, J. Schmidt, Lifetime degradation and regeneration in multicrystalline silicon under illumination at elevated temperature, AIP Adv. 6 (2016), http://dx.doi.org/10.1063/1.4944839.

[16] W. Shockley, W.T. Read, Statistics of the recombination of holes and electrons, Phys. Rev. 87 (1952) 835–842, http://dx.doi.org/10.1103/PhysRev.87.835.

[17] C. Vargas, Y. Zhu, G. Coletti, C. Chan, D. Payne, M. Jensen, Z. Hameiri, multicrystalline silicon for solar cells recombination parameters of lifetime-limiting carrier-induced defects in multicrystalline silicon for solar cells, Appl. Phys. Lett. 92106 (2017), http://dx.doi.org/10.1063/1.4977906.

[18] D.N.R. Payne, C.E. Chan, B.J. Hallam, B. Hoex, M.D. Abbott, S.R. Wenham, D.M. Bagnall, Rapid passivation of carrier-induced defects in p-type multi-crystalline silicon, Sol. Energy Mater. Sol. Cells 158 (2016) 102–106, http://dx.doi.org/10.1016/j.solmat.2016.05.022.

[19] T. Luka, S. Großer, C. Hagendorf, K. Ramspeck, M. Turek, Intra-grain versus grain boundary degradation due to illumination and annealing behavior of multi-crystalline solar cells, Sol. Energy Mater. Sol. Cells 158 (2016) 43–49, http://dx.doi.org/10.1016/j.solmat.2016.05.061.

[20] D. Sperber, A. Heilemann, A. Herguth, G. Hahn, Temperature and light induced changes in bulk and passivation quality of boron-doped float-zone silicon coated with SiNx:H, IEEE J. Photovolt. (2017) 1–8, http://dx.doi.org/10.1109/JPHOTOV.2017.2649601.

[21] F. Fertig, R. Lantzsch, A. Mohr, M. Schaper, M. Bartzsch, D. Wissen, F. Kersten, A. Mette, S. Peters, A. Eidner, J. Cieslak, K. Duncker, M. Junghänel, E. Jarzembowski, M. Kauert, D. Meißner, B. Reiche, S. Geißler, S. Hörnlein, C. Klenke, L. Niebergall, A. Schönmann, A. Weihrauch, F. Stenzel, A. Hofmann, T. Rudolph, A. Schwabedissen, M. Gundermann, M. Fischer, J.W. Müller, D.J.W. Jeong, Mass production of p-type Cz silicon solar cells approaching average stable conversion efficiencies of 22%, in: Proceedings of the 7th International Conference Silicon Photovoltaics, SiliconPV, ScienceDirect, 2017 (in press).

[22] N. Nampalli, H. Li, M. Kim, B. Stefani, S. Wenham, B. Hallam, M.D. Abbott, Multiple pathways for permanent deactivation of boron-oxygen defects in p-type silicon, in: Proceedings of the 7th International Conference Cryst. Silicon Photovoltaics, 2017 (in press).

[23] T. Niewelt, M. Selinger, N.E. Grant, W. Kwapil, J.D. Murphy, M.C. Schubert, Light-induced activation and deactivation of bulk defects in boron-doped float-zone silicon, J. Appl. Phys. 121 (2017) 185702, http://dx.doi.org/10.1063/1.4983024.

[24] Z. Hameiri, N. Borojevic, L. Mai, N. Nandakumar, K. Kim, S. Winderbaum, Should the Refractive Index at 633 nm be used to Characterize Silicon Nitride Films?, (2016) 2900–2904.

[25] Z. Hameiri, N. Borojevic, L. Mai, N. Nandakumar, K. Kim, S. Winderbaum, Low-absorbing and thermally stable industrial silicon nitride films with very low surface recombination, IEEE J. Photovolt. 7 (2017) 996–1003, http://dx.doi.org/10.1109/JPHOTOV.2017.2706424.

[26] H. Nagel, C. Berge, A.G. Aberle, H. Nagel, C. Berge, A.G. Aberle, Generalized analysis of quasi-steady-state and quasi-transient measurements of carrier lifetimes in semiconductors generalized analysis of quasi-steady-state and quasi-transient measurements of carrier lifetimes in semiconductors, J. Appl. Phys. 86 (1999) 6218–6221, http://dx.doi.org/10.1063/1.371633.

[27] A. Richter, F. Werner, A. Cuevas, J. Schmidt, S.W. Glunz, Improved parameterization of Auger recombination in silicon, Energy Procedia 27 (2012) 88–94, http://dx.doi.org/10.1016/j.egypro.2012.07.034.

[28] S.W. Glunz, S. Rein, W. Warta, J. Knobloch, W. Wettling, Degradation of carrier lifetime in Cz silicon solar cells, Sol. Energy Mater. Sol. Cells 65 (2001) 219–229, http://dx.doi.org/10.1016/S0927-0248(00)00098-2.

[29] N. Nampalli, T.H. Fung, S. Wenham, B. Hallam, M. Abbott, Statistical analysis of recombination properties of the boron-oxygen defect in p-type Czochralski silicon, Front. Energy 11 (2017) 4–22, http://dx.doi.org/10.1007/s11708-016-0442-6.

[30] K. Bothe, J. Schmidt, Electronically activated boron-oxygen-related recombination centers in crystalline silicon, J. Appl. Phys. 99 (2006), http://dx.doi.org/10.1063/1.2140584.

[31] B. Lim, F. Rougieux, D. Macdonald, K. Bothe, J. Schmidt, Generation and annihilation of boron? Oxygen-related recombination centers in compensated p- and n-type silicon, J. Appl. Phys. 108 (2010) 103722, http://dx.doi.org/10.1063/1.3511741.

[32] N.E. Grant, F.E. Rougieux, D. MacDonald, J. Bullock, Y. Wan, Grown-in defects limiting the bulk lifetime of p -type float-zone silicon wafers, J. Appl. Phys. 117 (2015) 0–8, http://dx.doi.org/10.1063/1.4907804.

[33] D. Macdonald, A. Cuevas, The trade-off between phosphorus gettering and thermal degradation in multicrystalline silicon, in: Proceedings of the 16th European Photovoltaic Solar Energy Conference, (2000) 1707–1710.

[34] J.F. Lelièvre, J. Hofstetter, A. Peral, I. Hoces, F. Recart, C. Del Cañizo, Dissolution and gettering of iron during contact co-firing, Energy Procedia 8 (2011) 257–262, http://dx.doi.org/10.1016/j.egypro.2011.06.133.

[35] M. Kim, P. Hamer, H. Li, D. Payne, S. Wenham, M. Abbott, B. Hallam, Impact of thermal processes on multi-crystalline silicon, Front. Energy 11 (2017) 32–41, http://dx.doi.org/10.1007/s11708-016-0427-5.

[36] D. Macdonald, A. Cheung, A. Cuevas, Gettering and poisoning of silicon wafers by phosphorus diffused layers, in: Proceedings of the 3rd World Conference on Photovoltaic Energy Conversion, 2 (2003) 11–14.

[37] B. Michl, J. Schön, W. Warta, M.C. Schubert, The impact of different diffusion temperature profiles on iron concentrations and carrier lifetimes in multicrystalline silicon wafers, IEEE J. Photovolt. 3 (2013) 635–640, http://dx.doi.org/10.1109/JPHOTOV.2012.2231726.

[38] F. Kersten, P. Engelhart, H.-C. Ploigt, A. Stekolnikov, T. Lindner, F. Stenzel, M. Bartzsch, A. Szpeth, K. Petter, J. Heitmann, J.W. Müller, Degradation of multicrystalline silicon solar cells and modules after illumination at elevated temperature, Sol. Energy Mater. Sol. Cells 142 (2015) 83–86, http://dx.doi.org/10.1016/j.solmat.2015.06.015.

[39] T.H. Fung, C.E. Chan, B.J. Hallam, D.N.R. Payne, M.D. Abbott, S.R. Wenham, Impact of annealing on the formation and mitigation of carrier-induced defects in multi-crystalline silicon, in: Proceedings of the 7th International Conference Silicon Photovoltaics, SiliconPV, 2017 (in press).

[40] P. Hamer, B. Hallam, S. Wenham, M. Abbott, Manipulation of hydrogen charge states for passivation of P-type wafers in photovoltaics, IEEE J. Photovolt. 4 (2014) 1252–1260, http://dx.doi.org/10.1109/JPHOTOV.2014.2339494.

[41] S. Martinuzzi, I. Périchaud, F. Warchol, Hydrogen passivation of defects in multicrystalline silicon solar cells, Sol. Energy Mater. Sol. Cells 80 (2003) 343–353, http://dx.doi.org/10.1016/j.solmat.2003.08.015.

[42] F. Kersten, J. Heitmann, J.W. Müller, Influence of Al2O3 and SiNx Passivation Layers on LeTID, Energy Procedia 92 (2016) 828–832, http://dx.doi.org/10.1016/j.egypro.2016.07.079.

[43] M. Sheoran, D.S. Kim, A. Rohatgi, H.F.W. Dekkers, G. Beaucarne, M. Young, S. Asher, Hydrogen diffusion in silicon from PECVD silicon nitride, in: Proceedings of the 2008 33rd IEEE Photovoltaic Specialists Conference, IEEE, (2008) 1–4. http://

dx.doi.org/10.1109/PVSC.2008.4922638.
[44] J.F. Lelièvre, E. Fourmond, A. Kaminski, O. Palais, D. Ballutaud, M. Lemiti, Study of the composition of hydrogenated silicon nitride SiNx:H for efficient surface and bulk passivation of silicon, Sol. Energy Mater. Sol. Cells 93 (2009) 1281–1289, http://dx.doi.org/10.1016/j.solmat.2009.01.023.
[45] J. Hong, W.M.M. Kessels, W.J. Soppe, A.W. Weeber, W.M. Arnoldbik, M.C.M. van de Sanden, Influence of the high-temperature ?Firing? Step on high-rate plasma deposited silicon nitride films used as bulk passivating antireflection coatings on silicon solar cells, J. Vac. Sci. Technol. B Microelectron. Nanometer Struct. 21 (2003) 2123, http://dx.doi.org/10.1116/1.1609481.
[46] G. Dingemans, W. Beyer, M.C.M. van de Sanden, W.M.M. Kessels, Hydrogen induced passivation of Si interfaces by Al2O3 films and SiO2/Al2O3 stacks, Appl. Phys. Lett. 97 (2010) 152106, http://dx.doi.org/10.1063/1.3497014.
[47] S. Wilking, S. Ebert, A. Herguth, G. Hahn, Influence of hydrogen effusion from hydrogenated silicon nitride layers on the regeneration of boron-oxygen related defects in crystalline silicon, J. Appl. Phys. 114 (2013) 194512, http://dx.doi.org/10.1063/1.4833243.
[48] K. Krauß, F. Fertig, D. Menzel, S. Rein, Light-induced degradation of silicon solar cells with aluminiumoxide passivated rear side, Energy Procedia 77 (2015) 599–606, http://dx.doi.org/10.1016/j.egypro.2015.07.086.
[49] T. Luka, C. Hagendorf, M. Turek, Multicrystalline PERC solar cells: is light-induced degradation challenging the efficiency gain of rear passivation? Photovolt. Int. 32 (2016) 37–44.
[50] T. Luka, S. Eiternick, S. Frigge, C. Hagendorf, H. Mehlich, M. Turek, Investigation of light induced degradation of multi-crystalline PERC cells, in: Proceedings of the 31st European Photovoltaic Solar Energy Conference and Exhibition, (2015) 826–828.
[51] F. Fertig, K. Krauß, S. Rein, Light-induced degradation of PECVD aluminium oxide passivated silicon solar cells, Phys. Status Solidi – Rapid Res. Lett. 9 (2015) 41–46, http://dx.doi.org/10.1002/pssr.201409424.
[52] B. Hallam, D. Chen, M. Kim, B. Stefani, B. Hoex, M. Abbott, S. Wenham, The role of hydrogenation and gettering in enhancing the efficiency of next-generation Si solar cells: an industrial perspective, Phys. Status Solidi 1 (2017) e201700305, http://dx.doi.org/10.1002/pssa.201700305.
[53] A. Cuevas, D. Macdonald, M. Kerr, C. Samundsett, A. Sloan, S. Shea, A. Leo, M. Mrcarica, S. Winderbaum, Evidence of impurity gettering by industrial phosphorus diffusion, in: Proceedings of the Conference Rec. Twenty-Eighth IEEE Photovolt. Spec. Conference – 2000 (Cat. No.00CH37036), IEEE, (2000) 244–247. http://dx.doi.org/10.1109/PVSC.2000.915803.
[54] V. Vähänissi, A. Haarahiltunen, H. Talvitie, M. Yli-Koski, H. Savin, Impact of phosphorus gettering parameters and initial iron level on silicon solar cell properties, Prog. Photovolt. Res. Appl. 21 (2013) 1127–1135, http://dx.doi.org/10.1002/pip.2215.
[55] A.E. Morishige, H.S. Laine, J. Schon, A. Haarahiltunen, J. Hofstetter, C. del Canizo, M.C. Schubert, H. Savin, T. Buonassisi, Building intuition of iron evolution during solar cell processing through analysis of different process models, Appl. Phys. A Mater. Sci. Process. 120 (2015) 1357–1373, http://dx.doi.org/10.1007/s00339-015-9317-7.
[56] P. Hamer, B. Hallam, M. Abbott, S. Wenham, Accelerated formation of the boron-oxygen complex in p-type Czochralski silicon, Phys. Status Solidi – Rapid Res. Lett. 9 (2015) 297–300, http://dx.doi.org/10.1002/pssr.201510064.
[57] B. Hallam, M. Abbott, T. Naerland, S. Wenham, Fast and slow lifetime degradation in boron-doped Czochralski silicon described by a single defect, Phys. Status Solidi – Rapid Res. Lett. 10 (2016) 520–524, http://dx.doi.org/10.1002/pssr.201600096.
[58] M. Kim, M. Abbott, N. Nampalli, S. Wenham, B. Stefani, B. Hallam, Modulating the extent of fast and slow boron-oxygen related degradation in Czochralski silicon by thermal annealing: evidence of a single defect, J. Appl. Phys. 121 (2017), http://dx.doi.org/10.1063/1.4975685.
[59] A. Inglese, A. Focareta, F. Schindler, J. Schön, J. Lindroos, M.C. Schubert, H. Savin, Light-induced degradation in multicrystalline silicon: the role of copper, Energy Procedia 92 (2016) 808–814, http://dx.doi.org/10.1016/j.egypro.2016.07.073.
[60] L.J. Geerligs, D. Macdonald, Dynamics of light-induced FeB pair dissociation in crystalline silicon, Appl. Phys. Lett. 85 (2004) 5227–5229, http://dx.doi.org/10.1063/1.1823587.
[61] J.E. Birkholz, K. Bothe, D. MacDonald, J. Schmidt, Electronic properties of iron-boron pairs in crystalline silicon by temperature- and injection-level-dependent lifetime measurements, J. Appl. Phys. 97 (2005), http://dx.doi.org/10.1063/1.1897489.
[62] X. Zhu, X. Yu, X. Li, P. Wang, D. Yang, Quantification of characteristic parameters for the dissociation kinetics of iron-boron pairs in Czochralski silicon, Scr. Mater. 64 (2011) 217–220, http://dx.doi.org/10.1016/j.scriptamat.2010.10.021.
[63] A. Herguth, G. Hahn, Boron-Oxygen Related Defects in Cz-Silicon Solar Cells Degradation, Regeneration and Beyond, 2 (2009) 974–976. http://dx.doi.org/10.4229/24thEUPVSEC2009-2AO.3.4.
[64] A. Herguth, G. Schubert, M. Kaes, G. Hahn, Investigations on the long time behavior of the metastable boron–oxygen complex in crystalline silicon, Prog. Photovolt. Res. Appl. 16 (2008) 135–140, http://dx.doi.org/10.1002/pip.779.